XXI IMEKO World Congress "Measurement in Research and Industry"
August 30 – September 4, 2015, Prague, Czech Republic

MEASUREMENT UNCERTAINTY OF ECHO PARAMETERS ESTIMATION IN UWB RADAR SYSTEM FOR MONITORING OF HUMAN MOVEMENTS

Paweł Mazurek, *Andrzej Miękina, Roman Z. Morawski*

Institute of Radioelectronics, Faculty of Electronics and Information Technology,
Warsaw University of Technology, Warsaw, Poland, email: R.Morawski@ire.pw.edu.pl

Abstract–The research reported in this paper is related to the ultra-wide-band radar technology that may be employed in care services for elderly and disabled persons. Two algorithms for preprocessing of measurement data from an impulse radar sensor, when applied for elderly people monitoring, are compared with respect to the uncertainty of estimation of echo parameters. Preliminary results of numerical experiments performed on those algorithms are demonstrated.

Keywords: UWB radar, healthcare, parameter estimation, measurement uncertainty

1. INTRODUCTION

The European and North-American populations are aging quickly. The problem of organised care over elderly people, especially those suffering dementia is, therefore, of increasing importance. Hence the demand for research on new technologies that could be employed in care services for such people. Its primary objective is to examine the applicability of various sensor systems for non-invasive monitoring of the movements and vital bodily functions, such as heart beat or breathing rhythm, of elderly persons in their home environment. There are three main categories of monitoring techniques already applied in care practice – wearable, environmental, vision-based – and three emerging categories: depth-camera-based (*cf.* the 2014 review paper [1]) and radar-based techniques (*cf.*, for example, the documents [2-13]). This paper is devoted to the latter ones, more precisely to the application of an ultra-wide-band (UWB) monostatic radar system for monitoring elderly and disabled people. The 2014 authors' papers, [14] and [15], contain key information on the organisation of such a system and on the envelope-based algorithms for preprocessing of measurement data acquired by that system. Here, two algorithms for estimation of radar echo parameters – an envelope-based algorithm and a new modified CLEAN algorithm – are compared with respect to the uncertainty of estimation.

2. PROBLEM STATEMENT

The shape of a pulse emitted by the radar sensor is usually modelled with a real-valued function $x(t)$, where t is a variable modelling time. The received signal, *i.e.* the response to $x(t)$, is modelled with a real-valued function $y(t)$. In Fig. 1 a digitalised version of the pulse $x(t)$ – *i.e.* a sequence $\{x_n\} = \{x(n\Delta t)\}$, where Δt is a sampling interval – is shown.

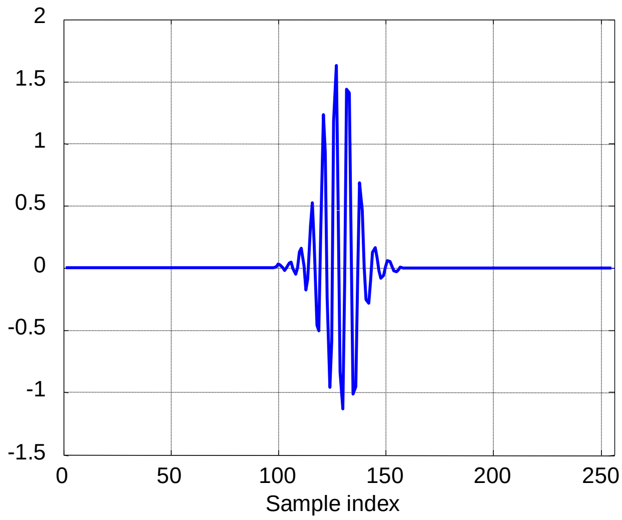

Fig. 1. Measured pulse emitted by the radar sensor.

Under the assumption that the emitted pulse is partially reflected from K surfaces located at different distances, the signal $y(t)$ may be given the form:

$$y(t) = \sum_{k=1}^{K} r_k \cdot x(t - t_k) \equiv r(t) * x(t) \tag{1}$$

where r_k $(k = 1, \ldots, K)$ are the reflection coefficients, t_k $(k = 1, \ldots, K)$ are time locations of the K echoes, and:

$$r(t) \equiv \sum_{k=1}^{K} r_k \cdot \delta(t - t_k) \tag{2}$$

For the sake of simplicity, the coefficients r_k will be called *magnitudes* and the time locations t_k will be called *positions* hereinafter.

The metrological performance of the following two algorithms for estimation of echo positions and magnitudes is compared:

– the max-envelope-based algorithm (called *ME algorithm*) which operates directly on the received data

sequence, and provides estimates of the positions and magnitudes of echoes, computed on the basis of its max-envelope;
- the modified CLEAN algorithm (called *MC algorithm*) which uses the cross-correlation function between the received data sequence and the template of the emitted pulse for estimation of the positions of echoes, and provides the least-squares estimates of their magnitudes.

The uncertainty of parameter estimation, attained by means of both algorithms, is evaluated in two test sets of semi-synthetic data generated on the basis of real-world data from an impulse radar sensor manufactured by Novelda SA.

3. METHODOLOGY OF NUMERICAL EXPERIMENTATION

3.1. Generation of semi-synthetic data

The study reported in this paper is based on the use of semi-synthetic measurement data. Sequences of such data, designed for testing purposes, have been generated according to formula:

$$\{\tilde{y}_n\} = \{y(n\Delta t)\} + \{\eta_n\} \text{ with } y(t) = \sum_{k=1}^{K} r_k \cdot x(t - t_k) \quad (3)$$

where $\{\eta_n\}$ is a sequence representative of the noise extracted from real-world data acquired by means of the radar sensor. In Fig. 2, an estimate of the standard deviation of the sensor noise, obtained on the basis of its $R = 4166$ recorded realisations, is presented.

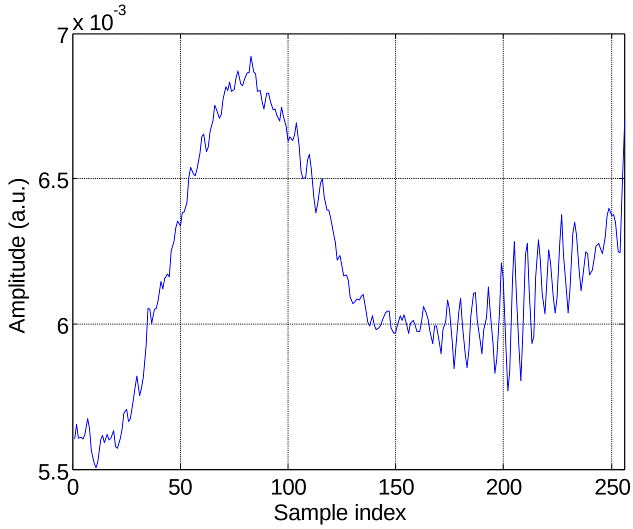

Fig. 2. Estimate of the standard deviation of the radar sensor noise, computed on the basis of its 4166 realisations.

The length of each sequence of data, used for experimentation, is the same as that of the window of observation in the radar sensor, *viz.* 256 samples. Since the sampling frequency is 3743561856 Hz, this window covers the distance of *ca.* 1 m.

3.2. Criteria for performance evaluation

Each experiment, completed using $R = 4166$ realisations of semi-synthetic data, has resulted in $2K$ sequences of estimates: $\{\hat{t}_k(n) | n = 1, \ldots, N\}$ and $\{\hat{r}_k(n) | n = 1, \ldots, N\}$ for $k = 1, \ldots, K$. The results of all experiments have been assessed using the following uncertainty indicators:

- the absolute standard deviation of the position estimates:

$$\hat{\sigma}_k^t = \sqrt{\frac{1}{N-1} \sum_{n=1}^{N} \left[\hat{t}_k(n) - \hat{\mu}_k^t\right]^2} \text{ for } k = 1, \ldots, K \quad (4)$$

where $\hat{\mu}_k^t$ is mean value of the position estimates for the k th echo;
- the absolute standard deviation of the magnitude estimates:

$$\hat{\sigma}_k^r = \sqrt{\frac{1}{N-1} \sum_{n=1}^{N} \left[\hat{r}_k(n) - \hat{\mu}_k^r\right]^2} \text{ for } k = 1, \ldots, K \quad (5)$$

where $\hat{\mu}_k^r$ is the mean value of the magnitude estimates for the k th echo.

The bias of the estimates has been neglected in performance evaluation since the inference procedures usually include computation of velocity and acceleration by numerical differentiation of the sequences of those estimates.

4. COMPAREDED ALGORITHMS

4.1. Max-envelope-based algorithm (ME algorithm)

The ME algorithm is almost the same as described in the paper [15]. Its sectioning part is composed of three steps:

- transformation of the original sequence of radar data $\{\tilde{y}_n\}$ into an auxiliary sequence of non-negative numbers $\{\tilde{y}_n^+\}$:

$$\{\tilde{y}_n^+\} \equiv \mathscr{F}_M\left[\{|\tilde{y}_n|\}; c, s\right] \quad (6)$$

where $\mathscr{F}_M[\circ; c, s]$ is the operator of Marmet filtering [16] with the parameters $c = 12$ and $s = 40$;
- determination of the envelope $\{y_n^E\}$ of the sequence $\{\tilde{y}_n^+\}$ according to the formula:

$$\{y_n^E\} = \mathscr{M}\left[\{\max(\tilde{y}_n^+ - y_{th}^{(0)}, 0)\}\right] \quad (7)$$

where $y_{th}^{(0)}$ is a discrimination level fit to the level of noise in the data $\{\tilde{y}_n\}$;
- determination of the borders between sections as points where the sequence $\{y_n^E\}$ has a minimum between two subsequent maxima:

$$n_k = \arg_n \min\left\{ y_n^E \,\middle|\, n = n'_k, \ldots, n'_{k+1} \right\} \quad (8)$$

where n'_k are ordered abscissas of all the maxima of the envelope, *i.e.*:

$$n'_k = \arg_n \max\left\{ \max(y_n^E - y_{th}^{(1)}, 0) \,\middle|\, n = 1, \ldots, N \right\} \quad (9)$$

for $k = 1, \ldots, K$ with $y_{th}^{(1)}$ being a discrimination level fit to the level of noise in the data $\{\tilde{y}_n^+\}$;
- supplementation of the set of minima abscissas with 1 and N.

For each section, defined by two consecutive minima, parameters of an echo – position and magnitude – are estimated according to the formulae:

$$t_k = \frac{m_{k1}}{m_{k0}} + n_k \quad (10)$$

$$r_k = m_{k0} \quad (11)$$

where:

$$m_{k0} = \sum_{n=n_k}^{n_{k+1}} y_n^E \quad (12)$$

$$m_{k1} = \sum_{n=n_k}^{n_{k+1}} \left[y_n^E \cdot (n - n_k + 1) \right] \text{ for } k = 1, \dots, K \quad (13)$$

4.2. Modified CLEAN algorithm (MC algorithm)

A preliminary examination of the basic CLEAN algorithm (known for *ca*. 40 years [17]), applied for estimation of the positions and magnitudes of echoes, demonstrated that it may be efficiently applied only for estimation of the echo positions, because the uncertainty of magnitude estimation is strongly dependent on the relative magnitudes of the echoes and the distance between them. Therefore, the algorithm has been modified and the magnitudes of the echoes are determined by means of the least-squares method.

In the description of the modified CLEAN algorithm, provided below, the following symbols are used:

$x(t)$ – emitted pulse;

$y(t)$ – received signal;

$\rho_{xx}(\tau)$ – non-normalised autocorrelation function of the emitted pulse $x(t)$;

$\rho_{\mathbf{yx}}(\tau)$ – non-normalised cross-correlation function between the emitted pulse $x(t)$ and received signal $y(t)$;

t_i – position of the echo found by the algorithm in the i th iteration;

T – constant offset between the maximum in the cross-correlation domain and the echo position in the time domain;

r_i – magnitude of the echo found by the algorithm in the i th iteration;

$y_i(t)$ – result of processing $y(t)$ by means of the CLEAN algorithm after the i th iteration;

ρ_{th} – threshold in the stopping criterion ($\rho_{\text{th}} > 0$);

γ – loop gain of the CLEAN algorithm ($\gamma \in (0, 1]$);

$\mathbf{y}$ – vector representation of the received $y(t)$; $\mathbf{y} \equiv [y_1 \dots y_N]^T$, $y_n \cong y(n \cdot \Delta t)$ for $n = 1, \dots, N$, $N = 256$;

$\mathbf{\Phi}$ – matrix containing shifted copies of the pulse $x(t)$; $\mathbf{\Phi} \equiv [\varphi_\mathbf{1} \ \dots \ \varphi_\mathbf{K}]$, $\varphi_k \equiv [x_1^k \ \dots \ x_N^k]^T$ $x_n^k \cong x(n \cdot \Delta t - t_k)$ for $n = 1, \dots, N$, $N = 256$; K – number of echoes found by the algorithm;

eem – vector of the estimates of the echo magnitudes.

The modified CLEAN algorithm comprises the following steps:

❶ $y_0(t) := 0$, $\rho_1(\tau) := \rho_{\mathbf{yx}}(\tau)$, $i := 1$;

❷ $\rho_{\max,i} := \max\{\rho_i(\tau)\}$, $\tau_i := \arg_\tau \max\{\rho_i(\tau)\}$;

❸ $\rho_{\max,i} < \rho_{\text{th}} \Rightarrow$ ❽;

❹ $t_i := \tau_i + T$, $r_i := \rho_{\max,i} / \max\{\rho_{xx}(\tau)\}$;

❺ $y_i(t) := y_{i-1}(t) + r_i \cdot x(t - t_i)$;

❻ $\rho_{i+1}(\tau) := \rho_i(\tau) - \gamma \cdot r_i \cdot \rho_{\text{xx}}(\tau - \tau_i)$;

❼ $i := i + 1, \Rightarrow$ ❷;

❽ $\mathbf{eem} := \mathbf{\Phi}^+ \mathbf{y}$.

5. NUMERICAL EXPERIMENTS

The performance of the algorithms has been evaluated using two test sets of semi-synthetic data. The first of them has contained data sequences representative of two strong echoes with magnitudes $m_1 = 1.0$ and $m_2 = m_1 / k$ (an example in Fig. 3); while the second has grouped data sequences representative of two echoes having weak magnitudes, *viz*. $m_1 = 0.1$ and $m_2 = m_1 / k$ (an example in Fig. 4). In both cases $k = 1, \dots, 5$, the position of the first echo has been fixed to $t_1 = 50$ while the position of the second to $t_2 = t_1 + dt$ for $dt = 0, 1, \dots, 150$. For each value of the distance dt, the performance indicators, defined in Subsection 3.2, have been calculated for $R = 4166$ realisations of the data. The experiment based on the first set of data has been labelled EXP1, the experiments based on the second – EXP2.

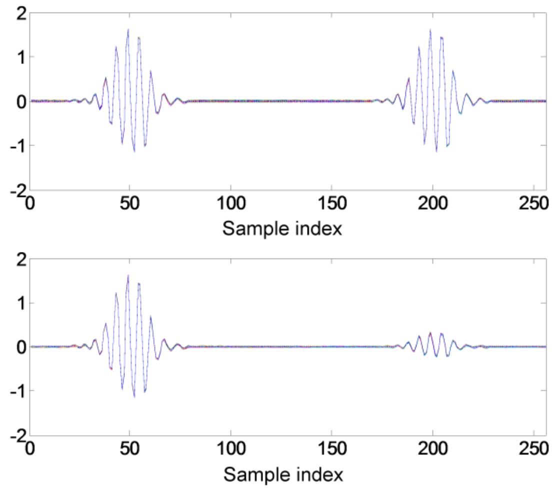

Fig. 3. Data sequences used in the experiment EXP1:
for the magnitude ratio m_1/m_2 = 1 (top),
for the magnitude ratio m_1/m_2 = 5 (bottom).

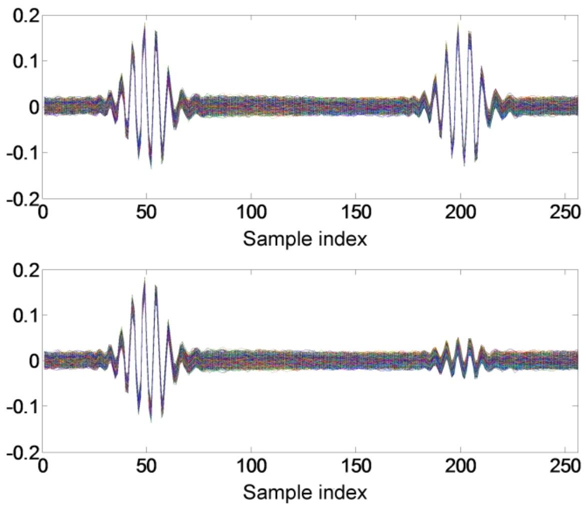

Fig. 4. Data sequences used in the experiment EXP2:
for the magnitude ratio $m_1/m_2 = 1$ (top),
for the magnitude ratio $m_1/m_2 = 5$ (bottom).

5.1. Experiment EXP1

The dependence of the absolute standard deviation of the position estimate of the stronger echo on the distance between echoes is shown in Fig. 5; the same for the position estimate of the weaker echo is provided in Fig. 6. In case of the ME algorithm, both standard deviations decrease when the distance between echoes is growing from 0 to 45 samples, and stabilise at the level of *ca*. 0.02 for the stronger echo and *ca*. 0.05 for the weaker echo. On the other hand, for the MC algorithm the absolute standard deviation of the estimate of the position is zero for both echoes, regardless of the distance between them.

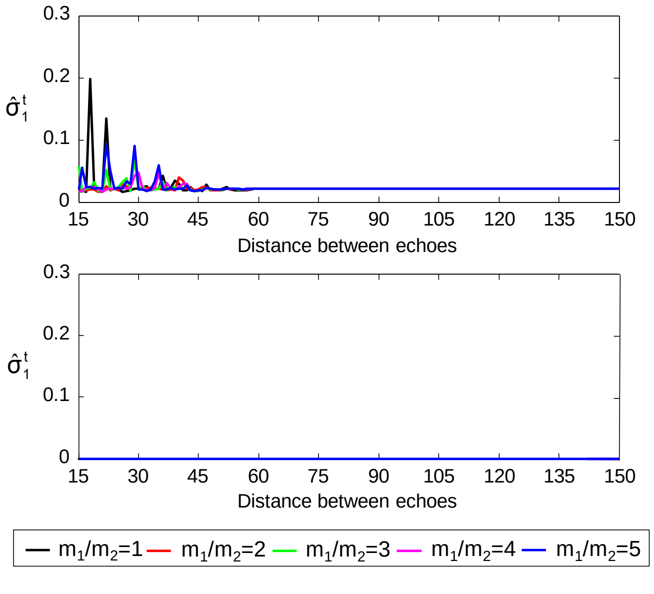

Fig. 5. Absolute standard deviation of the estimate of the stronger echo position in the experiment EXP1:
for the ME algorithm (top) and for the MC algorithm (bottom).

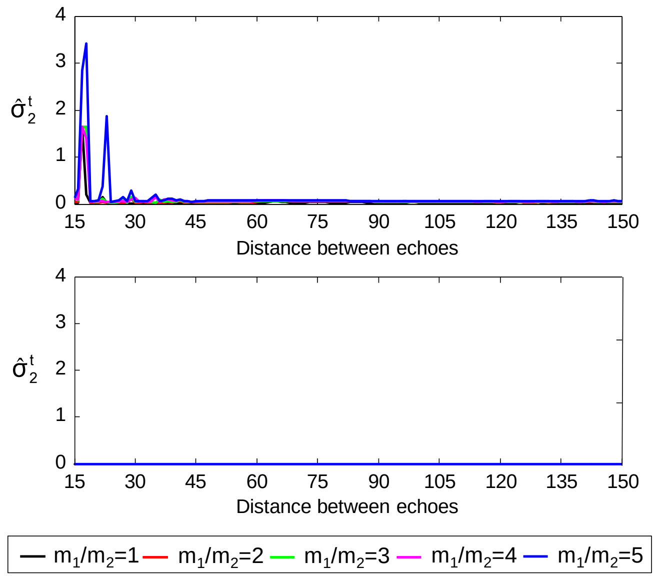

Fig. 6. Absolute standard deviation of the estimate of the weaker echo position in the experiment EXP1:
for the ME algorithm (top) and for the MC algorithm (bottom).

The dependence of the absolute standard deviation of the magnitude estimate of the stronger echo on the distance between echoes is shown in Fig. 7; the same for the magnitude estimate of the weaker echo is provided in Fig. 8. In case of the ME algorithm, both standard deviations decrease when the distance between echoes is growing from 0 to 40 samples, and stabilise at the level of *ca*. 0.03 if the distance is greater than 40 samples. For the MC algorithm, the standard deviation of the estimate of both echoes magnitudes oscillates around 0.0014, regardless of the distance between them.

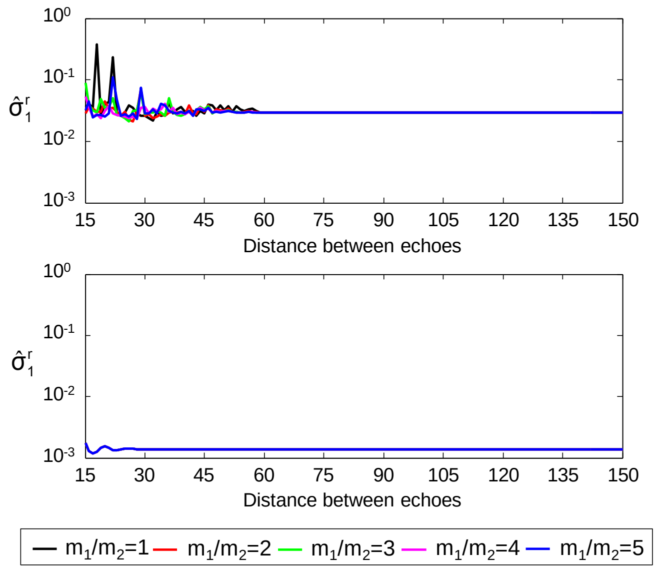

Fig. 7. Absolute standard deviation of the estimate of the stronger echo magnitude in the experiment EXP1:
for the ME algorithm (top) and for the MC algorithm (bottom).

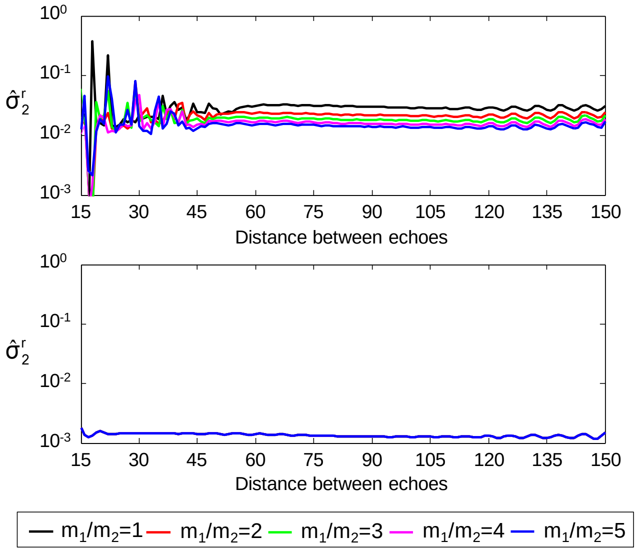

Fig. 8. Absolute standard deviation of the estimate of the weaker echo magnitude in the experiment EXP1: for the ME algorithm (top) and for the MC algorithm (bottom).

5.2. Experiment EXP2

The dependence of the absolute standard deviation of the position estimate of the stronger echo on the distance between echoes is shown in Fig. 9; the same for the position estimate of the weaker echo is provided in Fig. 10. It may be seen that for the ME algorithm the absolute standard deviation of the estimate of the position of both echoes is much larger than in the experiment EXP1. For the stronger echo, the standard deviation is reaching a minimum of 0.3-0.4 at the distance of *ca*. 30 samples, and is slowly growing for its larger values; for the weaker echo, it assumes very large values even for very distant echoes. On the other hand, for the MC algorithm, the absolute standard deviation of the estimate of the position is zero for both echoes, regardless of the distance between them.

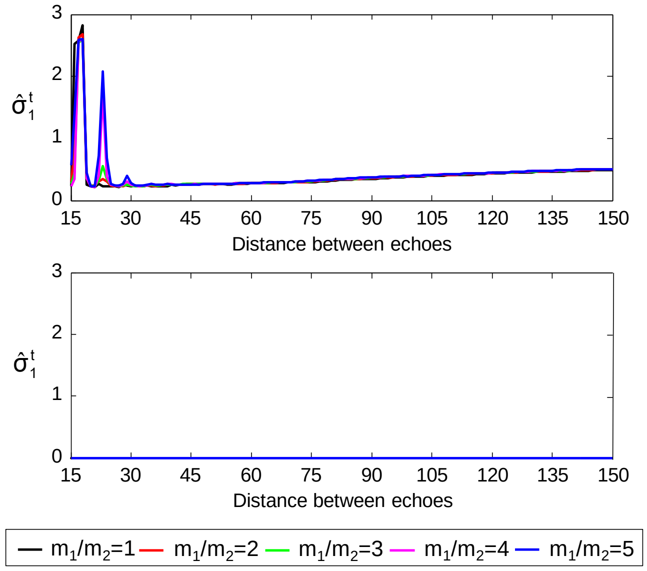

Fig. 9. Absolute standard deviation of the estimate of the stronger echo position in the experiment EXP2: for the ME algorithm (top) and for the MC algorithm (bottom).

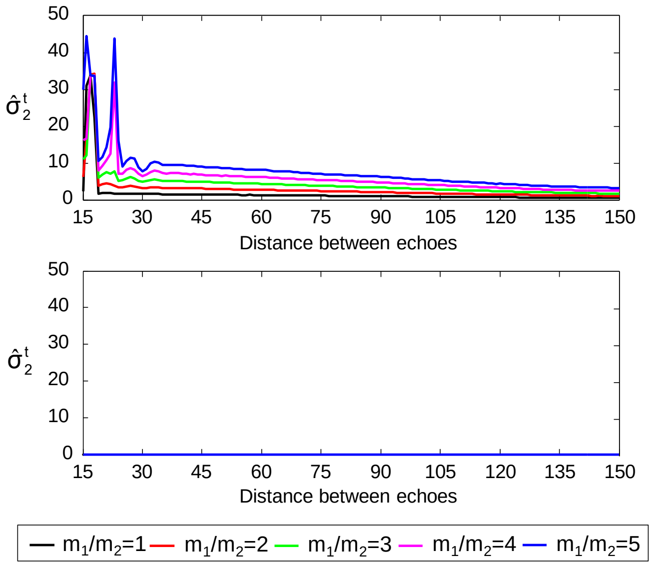

Fig. 10. Absolute standard deviation of the estimate of the weaker echo position in the experiment EXP2: for the ME algorithm (top) and for the MC algorithm (bottom).

The dependence of the absolute standard deviation of the magnitude estimate of the stronger echo on the distance between echoes is shown in Fig. 11; the same for the magnitude estimate of the weaker echo is provided in Fig. 12. It may be seen that the performance of both algorithms is similar to that in the experiment EXP1. For the ME algorithm, both standard deviations decrease when the distance between echoes is growing from 0 to 40 samples, and stabilise at the level of *ca*. 0.03 if the distance is greater than 40 samples. For the MC algorithm, the standard deviation of the estimate of both echoes magnitudes oscillates *ca*. 0.0014, regardless of the distance between them.

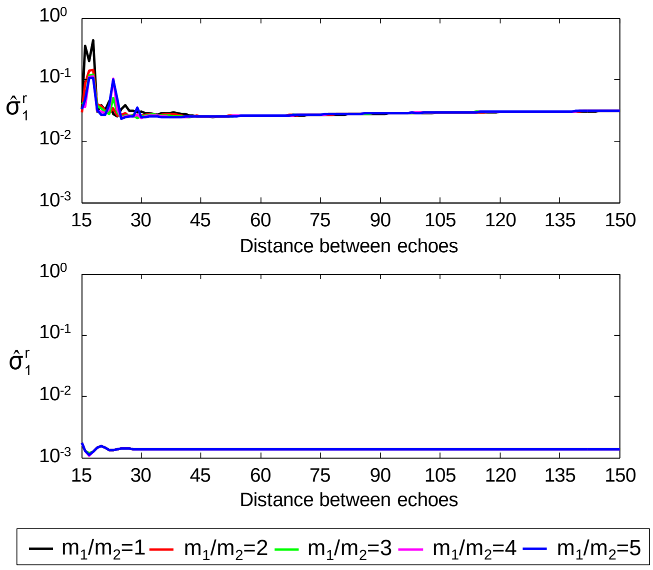

Fig. 11. Absolute standard deviation of the estimate of the stronger echo magnitude in the experiment EXP2: for the ME algorithm (top) and for the MC algorithm (bottom).

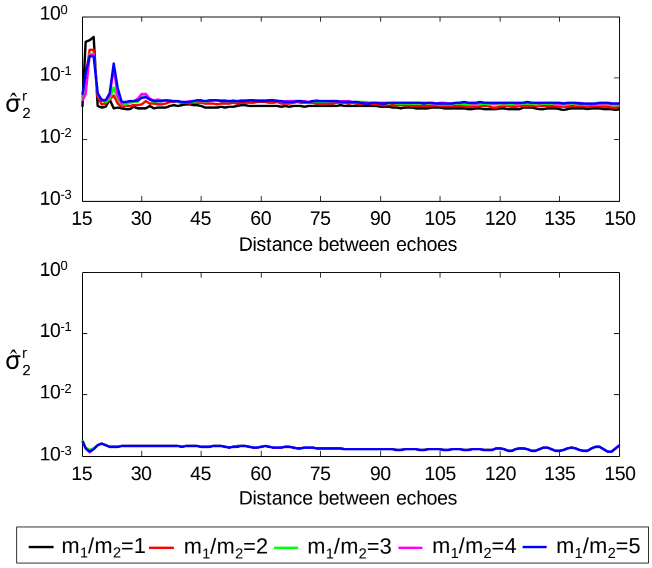

Fig. 12. Absolute standard deviation of the estimate of the weaker echo magnitude in the Experiment EXP2:
for the ME algorithm (top) and for the MC algorithm (bottom).

6. CONCLUSION

The performance of the max-envelope-based algorithm and the modified CLEAN algorithm has been compared with respect to measurement uncertainty, when applied for estimation of echo parameters in a radar-based system for monitoring of human movements. Two extensive numerical experiments, based on the semi-synthetic data, have shown the superiority of the MC algorithm both in terms of the level of uncertainty and its low sensitivity to the positions and magnitudes of echoes. This algorithm is able to determine the positions of both echoes with zero standard deviations, regardless of the ratio of their magnitudes and of the distance between them. Moreover, it is able to estimate the magnitudes of both echoes with the absolute standard deviation even 10 times smaller the ME algorithm.

ACKNOWLEDGMENTS

This work has been accomplished within the project PL12-0001 financially supported by *EEA Grants – Norway Grants* (*http://eeagrants.org/project-portal/project/PL12-0001*).

REFERENCES

[1] D. Webster, and O. Celik, "Systematic review of Kinect applications in elderly care and stroke rehabilitation," *Journal of Neuroengineering and Rehabilitation*, vol. 11, no. 108, pp. 1–24, 2014.

[2] B. Y. Su, K. C. Ho, M. Rantz, and M. Skubic, "Doppler Radar Fall Activity Detection Using The Wavelet Transform," *IEEE Transactions on Biomedical Engineering*, pp. 1–11, 2015.

[3] K. Stormo, *Human Fall Detection Using Distributed Monostatic UWB Radars*: M.Sc. Thesis, Department of Engineering Cybernetics, Norwegian University of Science and Technology, Trondheim, 2014.

[4] Qiuchi Jian, Jian Yang, Yinan Yu, P. Bjorkholm, and T. McKelvey, "Detection of Breathing and Heartbeat by Using a Simple UWB Radar System," *Proc. 8th European Conference on Antennas and Propagation*, pp. 3078–3081, 2014.

[5] Yazhou Wang, and A. E. Fathy, "UWB micro-doppler radar for human gait analysis using joint range-time-frequency representation," *Proc. SPIE. 'Active and Passive Signatures IV'*, vol. 8734, pp. 04.1–04.9, 2013.

[6] Xin Li, Dengyu Qiao, Ye Li, and Huhe Dai, "A Novel Through-Wall Respiration Detection Algorithm Using UWB Radar," *Proc. 35th Annual International Conference of the IEEE Engineering in Medicine and Biology Society*, pp. 1013–1016, 2013.

[7] M. Othman, M. Sinnappa, H. Azman, M. Aziz, M. Ismail, M. Hussein, H. Sulaiman, M. Misran, M. Said, R. Ramlee, J. Soh Ping, and B. Ahmad, "5.8 GHz Microwave Doppler Radar for Heartbeat Detection," *Proc. 23th Conference 'Radioelektronika'*, pp. 367–370, 2013.

[8] Meng Wu, Xiaoxiao Dai, Y. D. Zhang, B. Davidson, M. G. Amin, and J. Zhang, "Fall Detection Based on Sequential Modeling of Radar Signal Time-Frequency Features," *Proc. IEEE International Conference on Healthcare Informatics*, pp. 169–174 2013.

[9] D. P. Fairchild, and R. M. Narayanan, "Micro-doppler radar classification of human motions under various training scenarios," *Proc. SPIE. 'Active and Passive Signatures IV'*, vol. 8734, pp. 07.1–07.11, 2013.

[10] Chi-Hsuan Hsieh, Yi-Hsiang Shen, Yu-Fang Chiu, Ta-Shun Chu, and Yuan-Hao Huang, "Human respiratory feature extraction on an UWB radar signal processing platform," *Proc. IEEE International Symposium on Circuits and Systems*, pp. 1079–1082, 2013.

[11] Yinan Yu, Jian Yang, T. McKelvey, and B. Stoew, "A Compact UWB Indoor and Through-Wall Radar with Precise Ranging and Tracking," *International Journal of Antennas and Propagation*, vol. 2012, pp. 1–11, 2012.

[12] C. E. Phillips, J. Keller, M. Popescu, M. Skubic, M. Rantz, P. E. Cuddihy, and T. Yardibi, "Radar Walk Detection in the Apartments of Elderly," *Proc. 34th Annual International Conference of the IEEE Engineering in Medicine and Biology Society*, pp. 5863–5866, 2012.

[13] C. E. Phillips, *Walk Detection Using Pulse-Doppler Radar*: M.Sc. Thesis, Faculty of the Graduate School at the University of Missouri-Columbia, 2012.

[14] R. Z. Morawski, Y. Yashchyshyn, R. Brzyski, F. Jacobsen, and W. Winiecki, "On applicability of impulse-radar sensors for monitoring of human movements," *Proc. 20th IMEKO TC-4 International Symposium*, pp. 786–791, 2014.

[15] R. Z. Morawski, A. Miękina, and P. Bajurko, "Measurement data preprocessing in a radar-based system for monitoring of human movements," *Proc. IMEKO Joint TC1-TC7-TC13 Symposium*, pp. 1–6, 2014.

[16] R. Z. Morawski, "Numerical Determination of Marmet's Filter Parameters," *Review of Scientific Instruments*, vol. 53, no. 4, pp. 540–542, 1982.

[17] J. A. Högbom, "Aperture synthesis with a non-regular distribution of interferometer baselines," *Astronomy and Astrophysics Supplement*, vol. 15, pp. 417–426, 1974.